# HIGH-EFFICIENCY MULTILAYER-DIELECTRIC DIFFRACTION GRATINGS

*M. D. Perry* *D. Decker*

*R. D. Boyd* *B. W. Shore*

*J. A. Britten*

## Introduction

The ability to produce short laser pulses of extremely high power and high irradiance, as is needed for fast ignitor[1] research in inertial confinement fusion, places increasing demands on optical components such as amplifiers, lenses, and mirrors that must remain undamaged by the radiation. Amplifiers pose particular problems, because as pulses become shorter it becomes increasingly difficult to extract the stored energy without causing detrimental effects originating from the dependence of the refractive index $n = n_0 + n_2E^2I = n_0 + \gamma I$ on irradiance $I$. The higher refractive index in the center of an intense laser beam acts as a focusing lens. The resulting wavefront distortion, left uncorrected, eventually leads to catastrophic filamentation. Major advances in energy extraction and resulting increases in focused irradiance have been made possible by the use of chirped-pulse amplification (CPA), long used in radar applications and newly applied to optical frequencies.[2]

Optical-frequency CPA systems, typified by the schematic diagram in Fig. 1, begin with a mode-locked oscillator that produces low-energy seed pulses with durations of ten to a few hundred femtoseconds. As a result of the classical uncertainty relation between time and frequency, these short pulses have a very broad frequency distribution. A pair of diffraction gratings (or other dispersive elements) lengthens the laser pulse and induces a time-varying frequency (or chirp). Following amplification, diffraction gratings compress the pulse back to nearly the original duration. Typically a nanojoule, femtosecond pulse is stretched by a factor of several thousand and is amplified by as much as 12 orders of magnitude before recompression. By producing the short pulse only after amplification, this technique makes possible efficient extraction of energy from a variety of broadband solid state materials, such as Ti:sapphire,[3,4] alexandrite,[5] Cr:LiSAF,[6,7] and Nd:glass.[8,9]

## Constraints on Gratings for CPA

Achieving high focused irradiance from a pulse ultimately requires both high peak power and excellent beam quality. There is therefore a demand for diffraction gratings that produce a high-quality diffracted wavefront, have high diffraction efficiency, and exhibit a high threshold for laser damage. With careful attention to control of linear and nonlinear aberrations in the lasing medium, and with the addition of a deformable mirror to the beam transport system to correct for other wavefront aberrations, it should be possible to produce nearly diffraction-limited petawatt pulses.

The grating pairs used for pulse compression are typically planar reflection gratings that direct the first-order ($m = -1$) diffraction nearly back along the incident direction, as occurs at the Littrow angle.[10] It is important that the gratings send almost all of the radiation into this order. The need for high efficiency follows from the fact that the beam is diffracted by a grating four times in a typical double-pass pulse compressor. Thus a grating whose diffraction efficiency is $\eta$ gives a maximum compressor efficiency (for double-pass compression) of $\eta^4$. As a result of this quartic dependence, even a small increase in grating efficiency provides a large increase in the energy output from the pulse compressor. With a typical diffraction efficiency into the $m = -1$ order of 86%, the maximum compressor efficiency is approximately 55%. By increasing the grating efficiency to 95%, one can achieve compressor efficiencies of over 80%. We have recently achieved nearly this theoretical limit with a record double-pass compressor throughput of 78%.

Commercial gratings[11] are often replicas, in which a master grating structure is reproduced on a secondary substrate and then given a thin metal coating to achieve high diffraction efficiency. High-quality master gratings for optical frequencies are produced mechanically, by ruling the grating pattern into a metal blank, or

holographically, by exposing a substrate coated with photoresist to a stable interference pattern, developing the latent image, and overcoating with a metal layer. Carefully designed metal-coated master and replica gratings have achieved diffraction efficiencies as high as 95% in the $m = -1$ order.[12,13] High-quality commercial metallic gratings more commonly have diffraction efficiencies of 80 to 92%.

For high-power lasers, the damage threshold of a grating is as important as its diffraction efficiency. In pulse compression, the damage threshold limits the amount of energy that can be tolerated in the pulse for a given grating area. The low damage threshold of diffraction gratings is responsible for their limitation to use in low-power tunable oscillators. Narrow-linewidth, grating-cavity laser systems based on broadband solid state materials such as Ti:sapphire, alexandrite, and Cr:LiSAF require gratings exhibiting damage thresholds above 2 J/cm$^2$ to access the high energy storage capacity of these materials.

Unfortunately, metallic diffraction gratings, whether produced by mechanical ruling or holographic techniques, have an inherently low threshold for optical damage due to optical absorption. Energy deposited into a thin surface layer (the skin depth) will raise the surface temperature, eventually to the boiling point, unless it is conducted away more rapidly than it arrives. The theoretical damage threshold[12] for metallic (gold) gratings operating in the region 700–1100 nm is less than 1.5 J/cm$^2$ for nanosecond pulses and less than 0.6 J/cm$^2$ for picosecond pulses. Our holographically produced gold-coated master gratings[12] exhibit damage thresholds for 1053-nm radiation of approximately 1.2 J/cm$^2$ for nanosecond pulses and 0.4 J/cm$^2$ for subpicosecond pulses. These values are near the theoretical maximum and are a factor of two higher than those available with commercial gratings.

Dielectric materials offer the potential for significantly higher optical damage thresholds than those of metals. At a laser wavelength of 1053 nm, fused silica exhibits

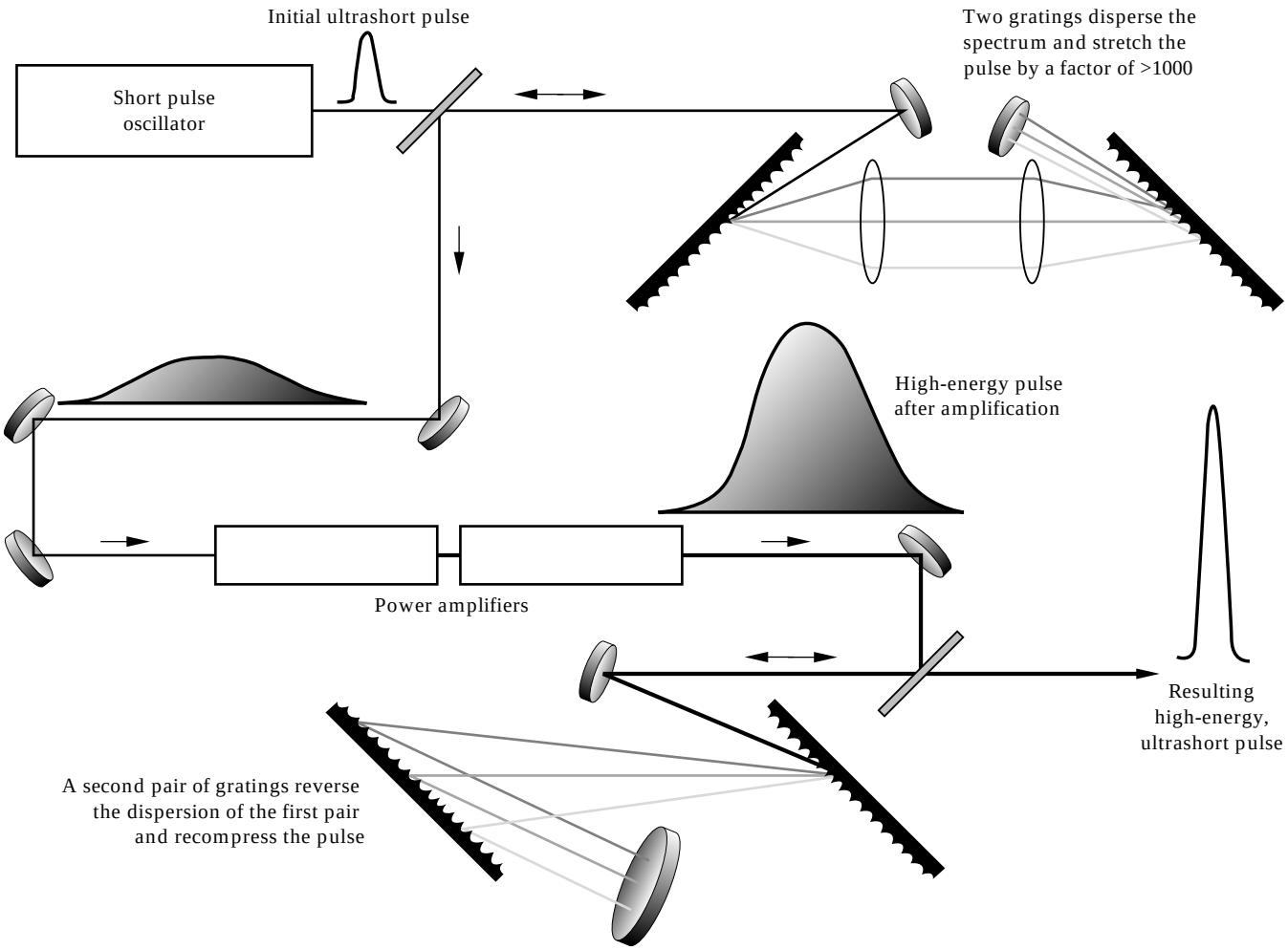


FIGURE 1. Partial schematic of beam stretching, amplifying, and compressing system used in high-power chirped pulse amplification (CPA), showing location of gratings and their function—giving different beams longer or shorter paths to stretch or compress the pulse.
(70-60-0695-1670pb01)

a damage threshold above 40 J/cm$^2$ for 1-ns pulses and above 2 J/cm$^2$ for 400-fs pulses.[14] Dielectric transmission gratings exhibiting high diffraction efficiency have been produced.[15] Unfortunately, the efficiency of these gratings in reflection is poor. In this article, we describe the design and performance of multilayer dielectric gratings that can achieve up to 98% diffraction efficiency in reflection in the $m = -1$ order, and that exhibit damage thresholds higher than those achievable with metallic gratings.

## Basic Grating Considerations

The basic geometric properties of any planar grating follow from the grating equation, which expresses the condition for constructive interference from successive periodic elements on a surface and which relates the incident angle $\theta_i$, the diffracted angle $\theta_m$ for order $m$, and the ratio of wavelength $\lambda$ to groove spacing $d$:

$$\sin\theta_m = \sin\theta_i + m\lambda/d. \quad (1)$$

Although these few parameters control the possible presence and direction of various diffracted orders, the distribution of energy among the orders (quantified by the grating efficiency) is determined by the wavelength and polarization of the incident light, the depth and shape of the grooves, and the optical properties of the diffracting structure. The groove profile depends on the method of manufacture and differs between ruled gratings (triangular profiles), holographic gratings (typically sinusoidal profiles) and etched lamellar gratings (rectangular or fin-shaped profiles).

For a reflection grating used in a first-order Littrow mount, the angle of incidence is fixed by the condition $\sin\theta_i = \lambda/2d$. When $\lambda/d > 2$, only specular reflection ($m = 0$) and evanescent orders occur; for $2 > \lambda/d > 2/3$, two propagating orders occur (specular reflection, $m = 0$, and retrodiffraction, $m = -1$). This latter two-order regime accounts for nearly all high-power laser applications.

Our grating designs are based on a rigorous solution of Maxwell's equations (with appropriate boundary conditions) for diffraction from a multilayer structure with a periodic surface-relief profile as shown in Fig. 2. We idealize the radiation as a monochromatic plane wave, linearly polarized as either transverse electric, TE (electric field along the grooves), or transverse magnetic, TM (magnetic field along the grooves). The grating profile can be of arbitrary shape, and the dielectric layers are specified by the layer thickness and an index of refraction. Our computations use the multilayer modal method.[16–19] This method replaces the corrugated grating surface by a succession of slices (rectangular in cross section), in each of which the complex-valued dielectric constant alternates periodically between two values, corresponding to the materials above and below the grating surface. Exact normal-mode solutions to the vector Helmholtz equation are found within the slices (an eigenvalue problem), and boundary conditions are matched in moment form to produce a complete solution. Solutions are carried between layers using an R-matrix method. The mathematical methods employed are discussed in detail elsewhere.[12,18,19]

Figure 3 presents the predicted $m = -1$ diffraction efficiency of a 1550-groove/mm grating used at the Littrow angle (56°) for TE-polarized 1053-nm light incident on the multilayer structure of Fig. 2. The multilayer is composed of alternating layers of high-index ZnS ($n = 2.35$) and low-index $ThF_4$ ($n = 1.52$) to form a highly reflecting quarter-wave stack. The top layer, containing the grating, is composed of the high-index (ZnS) layer. High diffraction efficiency is achieved by controlling the thickness $t$ of the top layer and the depth $h$ of the trapezoidal grooves. The maximum diffraction efficiency (predicted to be above 98%) occurs for an infinite periodic series of choices for $t$. To simplify fabrication, we always choose the thinnest solution.

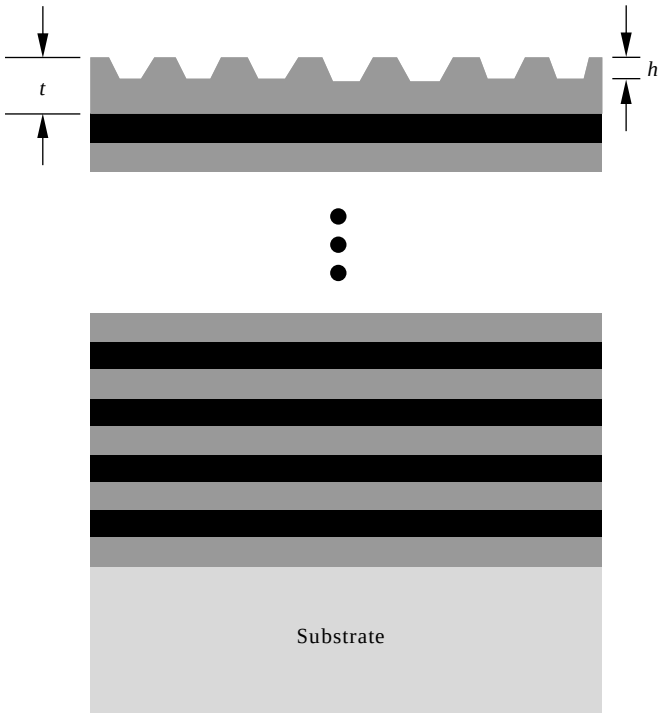


FIGURE 2. Basic multilayer dielectric grating concept ($h$ = groove depth, $t$ = top layer thickness). Dark and light layers represent materials of high ($n \approx 2$) and low ($n \approx 1.5$) refractive index, respectively. (70-60-0695-1667pb01)

Figure 3 gives a detailed view of the diffraction efficiency as a function of $h$ and $t$. Strong diffraction occurs when the optical depth of the grooves is near one quarter of a wavelength and the optical thickness of the top layer is near three quarters of a wavelength. Our calculations suggest high sensitivity to the incident polarization, as might be expected from the polarization sensitivity of conventional multilayer coatings. The peak diffraction efficiency for TM (p-polarized) light on this structure is predicted to be less than 50%; that for TE (s-polarized) light is predicted to be near 98%.

## Manufacturing Procedure

Our gratings are fabricated using lithographic techniques following holographic exposure. The dielectric multilayer structure is vacuum-deposited by e-beam evaporation on an optically flat (better than $\lambda/12$) substrate. The substrate is then coated with a thin (~300 nm) film of photoresist (Shipley 1400) and cured at 80°C for 30 min. The surface relief pattern spacing $d$ is produced in the photoresist by intersecting two laser beams, each of exposure wavelength $\lambda_e$ and each incident at an angle $\theta_e$ according to the formula

$$d = \frac{\lambda_e}{2 \sin \theta_e \cos \phi} \quad , \tag{2}$$

where $\phi$ is the angle between the normal to the substrate and the bisector of the incident laser beams (see Fig. 4). The interference pattern was produced by an equal-path, fringe-stabilized interferometer utilizing a 2-W single-longitudinal-mode Kr-ion laser (Coherent) operating at 413 nm. Straight, parallel grooves are produced only by highly collimated radiation; even the slightest wavefront curvature of the interfering beams produces curved grooves with nonuniform spacing. This groove distortion reduces the spectral resolution of the grating and produces undesirable curvature in the wavefront of the diffracted beam.

Once the interference pattern is recorded in the photoresist, development removes those regions exposed to the laser light (positive resist), producing a corrugated surface relief profile that is transferred into the substrate material by reactive-ion etching.[19] Although the interference fringe pattern exhibits a sinusoidal intensity distribution, the groove shape ultimately produced in the grating is affected by a number of process variables. Our most common profile is trapezoidal, so we optimize the designs for trapezoidal grooves.

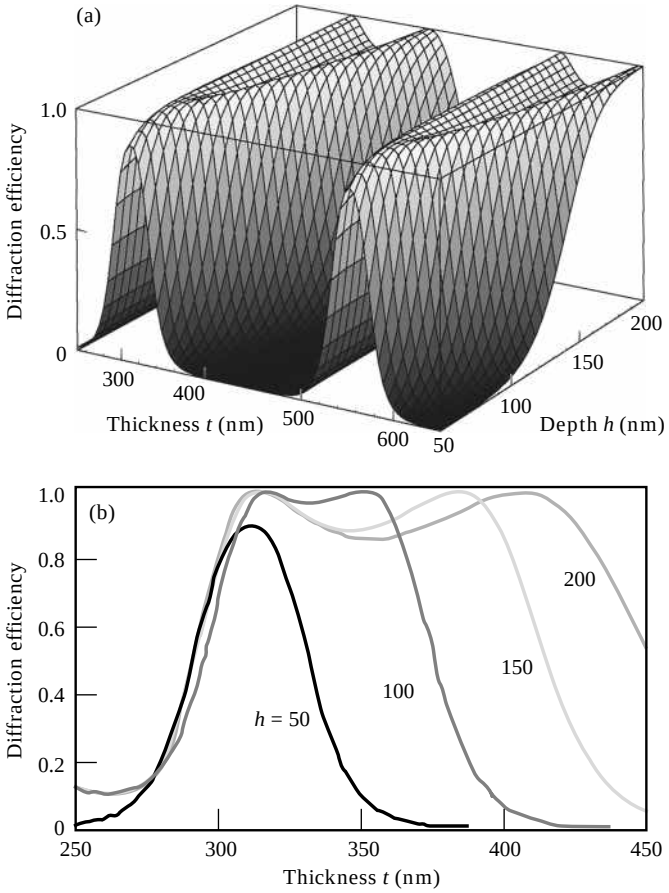


FIGURE 3. (a) Theoretical diffraction efficiency (order $m = -1$) for TE-polarized light at 1053 nm for a multilayer dielectric grating consisting of alternating layers of ZnS and $ThF_4$. Trapezoidal grooves are etched into the top layer as illustrated in Fig. 2. (b) Expanded view of first maxima of efficiency surface, showing efficiency (order $m = -1$) for depths $h$ = 50, 100, 150 and 200 nm. (70-60-0695-1668pb01)

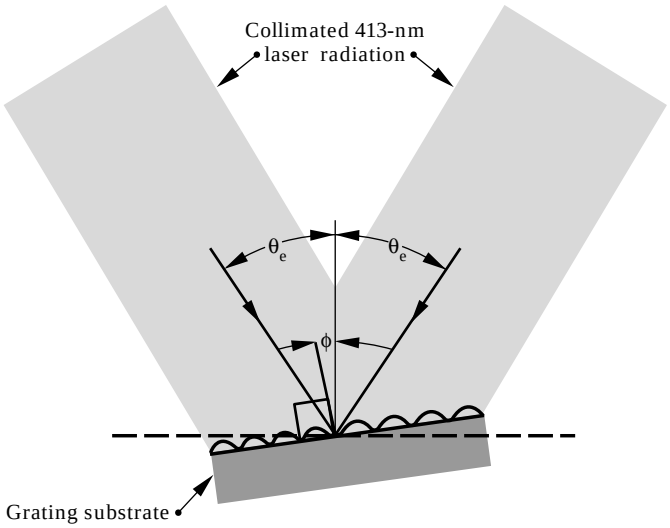


FIGURE 4. Holographic exposure geometry, showing definition of angle of incidence $\theta$ and angle $\phi$ between grating normal and bisector of incident waves. (70-60-0695-1669pb01)

Figure 5 shows a typical scanning electron micrograph of a cross section of a completed grating.

We determined the dependence of the diffraction efficiency of this grating on the angle of incidence by measuring the average power of the diffracted ($m = -1$, near the Littrow angle), reflected ($m = 0$), and incident beams produced by a narrow-linewidth Ti:sapphire cw laser operating at 1053 nm. Figure 6 shows the results of this measurement. The difference between the incident beam and the sum of the diffracted and reflected beams arises from a net scattering of ~1% and a transmission loss of ~0.5%. Low diffraction efficiency is observed until the design angle of 56° is approached; there the reflected ($m = 0$) energy for TE polarization drops to approximately 1% of the incident energy and the $m = -1$ diffracted beam reaches a peak efficiency of 96.1%. For TM polarization, the maximum diffraction efficiency is 50%, in good agreement with the predicted value. We observe a small variation of efficiency (from a high of 96% to a low of 94%) over the surface of our gratings.

The measured damage threshold of our oxide ($HfO_2/SiO_2$)–based multilayer dielectric gratings for 1-ns laser pulses is over 5 J/cm$^2$, nearly ten times that of the best metallic gratings. For pulse durations from 0.3 to 5 ps, our gratings exhibit a damage threshold of approximately 0.6 J/cm$^2$, three times higher than the short-pulse damage threshold of commercial metallic gratings. Further refinement of our multilayer design is expected to increase the short-pulse damage threshold to over 1 J/cm$^2$.

In addition to the requirement of high diffraction efficiency and high damage threshold, gratings used for pulse compression must maintain high efficiency over a large bandwidth. Figure 7 shows the calculated

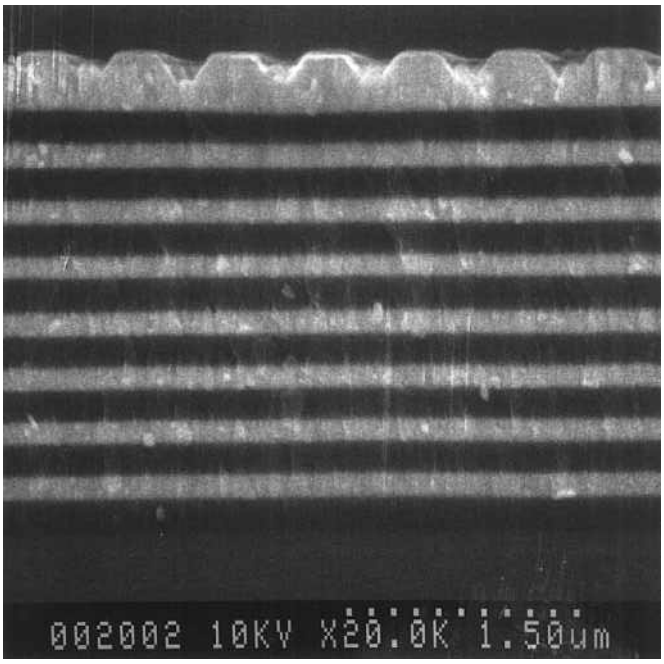


FIGURE 5. Scanning electron micrograph of multilayer dielectric grating structure. (20-03-0795-1855pb01)

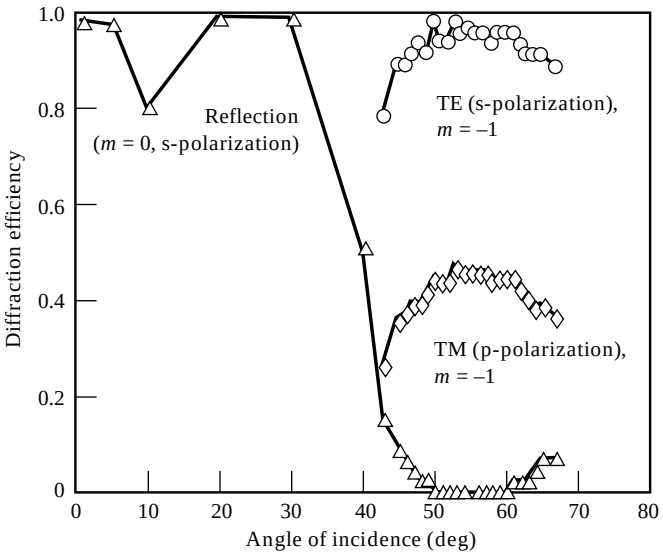


FIGURE 6. Absolute diffraction efficiency (order $m = -1$, Littrow mount) at a wavelength of 1053 nm and for various polarizations for the grating shown in Fig. 5. (70-60-0695-1671pb01)

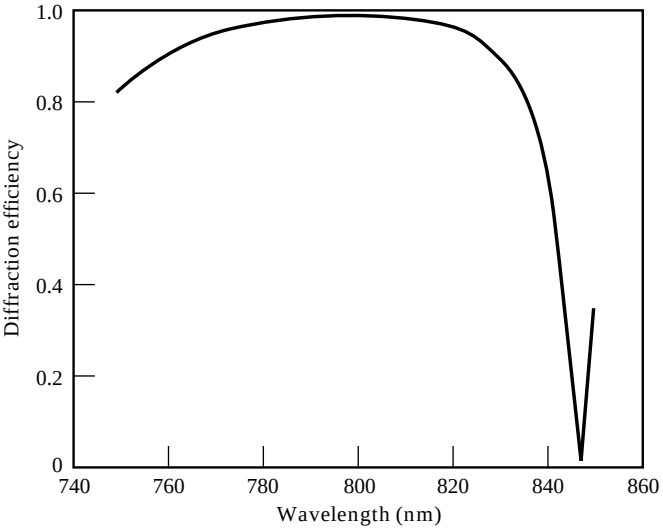


FIGURE 7. Theoretical diffraction efficiency ($m = -1$) vs wavelength of an oxide-based multilayer grating (1800 grooves/mm). Bandwidth is over 85 nm. (70-60-0695-1672pb01)

wavelength dependence of the diffraction efficiency of diffraction efficiency an oxide-based multilayer grating (8 layer pairs) optimized for use with 100-fs pulses at 800 nm. Diffraction efficiency above 90% is maintained from 760 to over 830 nm. Such gratings could easily handle pulses as short as 20 fs. We can increase the bandwidth, at the price of a slightly reduced peak diffraction efficiency, by reducing the number of layers or changing the design slightly. We have produced designs that can support pulses as short as 10 fs with greater than 90% diffraction efficiency. At these extremely short pulse durations, the dispersion of the multilayer coating itself will become important. We have not yet examined this effect on our ability to use these gratings for stretching and compressing 10-fs pulses.

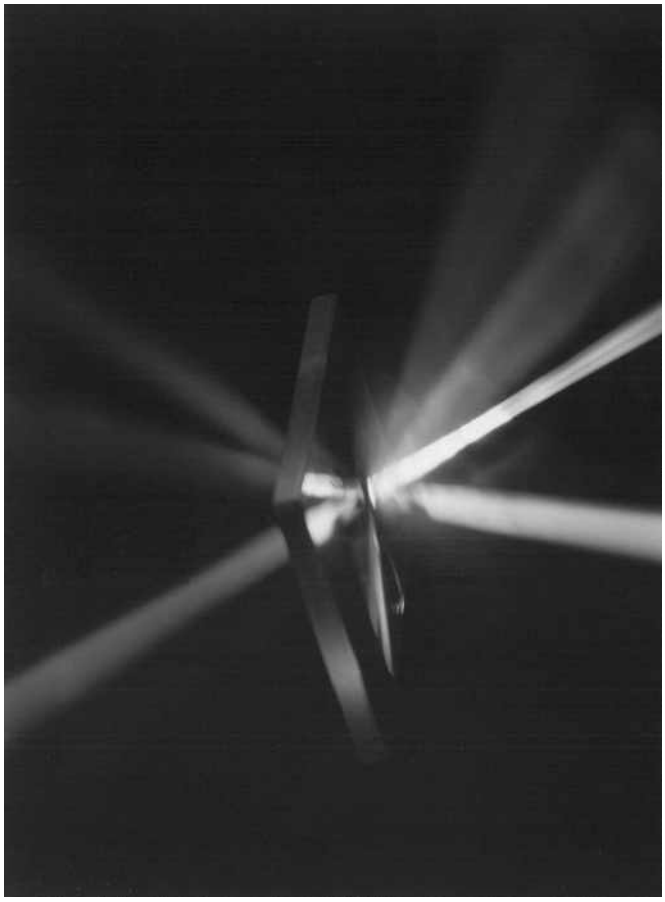

FIGURE 8. Multilayer dielectric diffraction grating designed to reflect yellow light, diffract broadband visible radiation (bottom left), eliminate all green and yellow light in the transmitted diffracted beam (right), and transmit blue–green light. The grating pictured is 15 × 20 cm. (70-15-0294-0178Apb01)

## Applications of Multilayer Dielectric Gratings

Another feature of this new type of diffraction grating is the ability to design the grating to perform a multitude of functions simultaneously. Specifically, the gratings can be designed as beamsplitters that transmit, diffract, and reflect light. By controlling the design of the multilayer and the grating, specific wavelengths can be transmitted, others reflected, and still others diffracted, all with specified efficiency. As an example, we fabricated a grating that operated simultaneously as a broadband diffraction grating in reflection (10% efficiency in the $m = -1$ order from 390 to 700 nm), a high reflector in the yellow (90% reflection from ~570 to 590 nm), a high transmitter in the blue-green (~90% from 500 to 570 nm), and a notch filter for the transmitted diffracted ($m = -1$) beam [extremely low efficiency (<1%) for 500 to 600 nm and relatively high efficiency (>50%) for 400 to 500 nm and 600 to 700 nm). Figure 8 displays this performance.

## Summary

We have demonstrated techniques for designing and holographically creating diffraction gratings, based on a multilayer dielectric structure, that exhibit diffraction efficiency exceeding 96% into the $m = -1$ order in a near-Littrow configuration. The high diffraction efficiency is obtained by proper coating design and by adjustment of the depth of the grooves and the thickness of the top layer. By adjusting the coating design, gratings of essentially any efficiency and variable bandwidth can be produced.

The damage thresholds of these all-dielectric gratings surpass those of metal gratings. To date, relative to commercial metallic diffraction gratings, our dielectric gratings have achieved an order-of-magnitude increase in damage threshold for nanosecond pulses and a factor-of-three increase for subpicosecond pulses.

## Acknowledgments

We thank E. Lindsay and C. Moore for producing the electron and atomic-force micrographs and C. Hoaglan for his technical assistance. We are indebted to Lifeng Li, of the University of Arizona, for ongoing advice and assistance.

## Notes and References


1. M. Tabak, J. M. Hammer, M. E. Glinsky, W. L. Kruer, et al., *ICF Quarterly Report* 4(3), 90–100, Lawrence Livermore National Laboratory, Livermore, CA, UCRL-LR-105821-94-3 (1994).
2. P. Maine, D. Strickland, P. Bado, M. Pessot, and G. Mourou, *IEEE J. Quantum Electron.* QE-24, 398–402 (1988).
3. J. Kmetec, J. J. Macklin, and J. F. Young, *Opt. Lett.* 16, 1001–3 (1991).
4. A. Sullivan, H. Hamster, H. C. Kapteyn, S. Gordon, *Opt. Lett.* 16, 1406–8 (1991).
5. M. Pessot, J. Squier, G. Mourou, and D. Harter, *Opt. Lett.* 14, 797–799 (1989); M. Pessot, J. Squier, P. Bado, G. Mourou, and D. Harter, *IEEE J. Quantum Electron.* QE-25, 61–66 (1989).
6. T. Ditmire and M. D. Perry, *Opt. Lett.* 18, 426–428 (1993); T. Ditmire, H. Nguyen, and M. D. Perry, *J. Opt. Soc. Amer. B* 11, 580 (1993).
7. P. Beaud, M. Richardson, E. J. Miesak, and B. H. T. Chai, *Opt. Lett.* 18, 1550–52 (1993).
8. M. D. Perry and R. Olson, *Laser Focus World* 27, 69 (1991).
9. C. Rouyer, E. Mazataud, I. Allais, A. Pierre, et al., *Opt. Lett.* 18, 214–216 (1993).
10. E. B. Treacy, *IEEE J. Quantum Electron.* QE-5, 454–8 (1969).
11. M. C. Hutley, *Diffraction Gratings* (Academic, NY, 1982).
12. R. Boyd, J. Britten, D. Decker, B. W. Shore, et al., *Appl. Opt.* 34, 1697 (1995).
13. E. Popov, L. Tsonev, and D. Maystre, *J. Mod. Opt.* 37, 367–377 (1990).
14. B. C. Stuart, M. D. Perry, and B. W. Shore, "Pulsewidth-Dependent Damage Measurements of Dielectric Materials," Lawrence Livermore National Laboratory, Livermore, CA, UCRL-JC-118115. Prepared for proceedings of *Physics with Intense Laser Pulses*, St. Malo, France, August 1994.
15. J. J. Armstrong, *Holographic Generation of Ultra-High-Efficiency Large-Aperture Transmission Diffraction Gratings* (Ph.D. Thesis, University of Rochester, 1993).
16. R. Petit, Ed. *Electromagnetic Theory of Gratings* (Springer, Berlin, 1980).
17. D. Maystre, "Rigorous Vector Theories of Diffraction Gratings," in *Progress in Optics*, E. Wolf, Ed. (Elsevier, NY, 1984), vol. 21, pp. 1–67.
18. L. Li, *J. Opt. Soc. Am. A* 10, 2581–91 (1993); L. Li, *J. Mod. Opt.* 40, 553–73 (1993); L. Li, *J. Opt. Soc. Am. A* 11, 2816–2828 (1994).
19. L. Li and C. W. Haggans, *J. Opt. Soc. Am. A* 10, 1184–1189 (1993).